

Covariant separable kernel of the deuteron

S. G. Bondarenko^a, V. V. Burov^a, W.-Y. Pauchy Hwang^b, E. P. Rogochaya^{a,*}

^a*Bogoliubov Laboratory of Theoretical Physics, Joint Institute for Nuclear Research,
Dubna, Russia*

^b*National Taipei University, Taipei 106, Taiwan*

Abstract

The six-rank separable kernel of the neutron-proton interaction for the triplet coupled ${}^3S_1^+$ - ${}^3D_1^+$ partial state within the covariant Bethe-Salpeter approach is constructed. Two different methods of a relativistic generalization of initially nonrelativistic form factors parametrizing the kernel are considered. Parameters of the kernel are defined from the description of phase shifts and low-energy characteristics in the elastic neutron-proton scattering. At the same time the half-off-shell behavior of the kernel is controlled by the appropriate description of the Noyes-Kowalski function and the deuteron properties.

Keywords: phase shifts, separable kernel, Bethe-Salpeter equation, neutron-proton elastic scattering, deuteron

PACS: 11.10.St, 11.80.Et, 13.75.Cs

1. Introduction

The deuteron has been an object of intensive investigations as the simplest system of the coupled neutron and proton. Throughout more than 40 years many methods for the description of the deuteron were elaborated [1]-[17]. The main goal of any approach is the description of the interaction between two nucleons in it. It is presented either by potentials in the Schrödinger

*Corresponding author. JINR, Joliot-Curie 6, 141980 Dubna, Moscow region, Russia. Tel.: +74962163503; fax: +74962165146

Email addresses: `bondarenko@jinr.ru` (S. G. Bondarenko), `burov@theor.jinr.ru` (V. V. Burov), `wyhwang@phys.ntu.edu.tw` (W.-Y. Pauchy Hwang), `rogoch@theor.jinr.ru` (E. P. Rogochaya)

equation or kernels in the Bethe-Salpeter (BS) equation. They are either constructed from the presentation of the interaction as an exchange by various mesons (realistic potentials [18, 19]) or presented as model functions which parameters are found from the description of observables in the elastic neutron-proton (np) scattering (separable [20]-[26] kernels, phenomenological kernels [27] etc). There are also alternative approaches [7, 15, 16], relativistic quantum mechanics, which are based on the Hamiltonian approach.

In respect of simplicity of performing calculations separable interaction kernels are the most convenient instrument if they are known [17]. That is why there are separable kernels intended only to reproduce the behavior of corresponding realistic potentials and used in calculations instead of more complicated originals (see, for example, [18] and [25]). However the construction of kernels of this type is a complicated problem. First elaborated kernels [20, 21] were nonrelativistic and therefore they were of little use for the description of reactions with high-energy particles. In addition there were problems with their off-shell behavior, see for example [22, 23]. This behavior was adjusted in subsequent models [24]-[26] by fitting to corresponding realistic potentials using the Ernst-Shakin-Thaler method [28]. However all these models do not contain the zero component of the momentum of considered particles which is necessary to construct a covariant model. One of attempts of this kind is [29] where the relativistically generalized version of Graz II kernel [24] was constructed. It describes the experimental data for the laboratory energies of the colliding neutron and proton T_{Lab} up to 0.5 GeV. However its application is limited in principle because of nonintegrability of expressions containing the form factors of this kernel [17] at higher T_{Lab} . The problem can be solved by using the modified form factors [30]. This idea was developed in our works [31]-[34] for the description of uncoupled partial states in the elastic np scattering for T_{Lab} up to 3 GeV.

In the presented paper the kernel for the triplet coupled np state $^3S_1^+ - ^3D_1^+$ is proposed. The work is a continuation of the previous one [34] where kernels for the description of uncoupled partial states with the total angular momenta $J = 0, 1$ are constructed. Using the elaborated kernel investigations of various deuteron characteristics are performed. Parameters of the kernel are defined from the calculations of experimental data for phase shifts taken from the SAID program (<http://gwdac.phys.gwu.edu>) and low-energy characteristics. The off-shell behavior of the kernel is compared with the deuteron wave function and the Noyes-Kowalski function [35, 36] obtained for some realistic potentials (here Paris, Bonn) which are very good at low energies.

The paper is organized as follows. In Sect.2, the general Bethe-Salpeter formalism used for the description of the np system is considered. In Sect.3, the solution of the BS equation with the separable interaction kernel is discussed. The constructed kernel is presented in Sect.4. The calculations of parameters of the kernel and obtained low-energy deuteron characteristics are presented in Sect.5. The review of the results for phase shifts of the elastic np scattering, components of the Noyes-Kowalski function, deuteron wave function and conclusions are performed in Sect.6.

2. Bethe-Salpeter formalism

Within the relativistic field theory, the elastic nucleon-nucleon (NN) scattering can be described by the scattering T matrix which satisfies the inhomogeneous Bethe-Salpeter equation [37]. In momentum space, the BS equation for the T matrix can be (in terms of the relative four-momenta p' and p and the total four-momentum P) represented as:

$$T(p', p; P) = V(p', p; P) + \frac{i}{4\pi^3} \int d^4k V(p', k; P) S_2(k; P) T(k, p; P), \quad (1)$$

where $V(p', p; P)$ is the interaction kernel and $S_2(k; P)$ is the free two-particle Green function

$$S_2^{-1}(k; P) = \left(\frac{1}{2} P \cdot \gamma + k \cdot \gamma - m\right)^{(1)} \left(\frac{1}{2} P \cdot \gamma - k \cdot \gamma - m\right)^{(2)},$$

γ are the Dirac gamma-matrices. The square of the total momentum $s = (p_1 + p_2)^2$ and the relative momentum $p = (p_1 - p_2)/2$ [$p' = (p'_1 - p'_2)/2$] are defined via the nucleon momenta p_1, p_2 [p'_1, p'_2] of initial [final] nucleons.

Performing the partial-wave decomposition (see details in [17, 34]) of the T matrix and interaction kernel V we can rewrite the BS equation for the off-shell partial-wave amplitudes:

$$\begin{aligned} T_{ab}(p'_0, |\mathbf{p}'|; p_0, |\mathbf{p}|; s) &= V_{ab}(p'_0, |\mathbf{p}'|; p_0, |\mathbf{p}|; s) \\ &+ \frac{i}{4\pi^3} \sum_{cd} \int_{-\infty}^{+\infty} dk_0 \int_0^{\infty} k^2 d|\mathbf{k}| V_{ac}(p'_0, |\mathbf{p}'|; k_0, |\mathbf{k}|; s) \\ &\times S_{cd}(k_0, |\mathbf{k}|; s) T_{db}(k_0, |\mathbf{k}|; p_0, |\mathbf{p}|; s). \end{aligned} \quad (2)$$

Here indices a, b etc denote the corresponding partial state quantum numbers $|aM\rangle \equiv |\pi, {}^{2S+1}L_J^\rho M\rangle$, where S is the total spin, L is the orbital angular

momentum, and J is the total angular momentum with the projection M ; relativistic quantum numbers ρ and π refer to the relative-energy and spatial parity with respect to the change of sign of the relative energy and spatial vector, respectively. The two-particle propagator S_{ab} depends only on ρ -spin indices.

Calculating the T matrix we can connect the parameters of the internal kernel with observables. For the description of the T matrix we use the following normalization condition in the on-mass-shell form for the triplet state:

$$T_{ll}(s) = \frac{i8\pi}{\sqrt{s}\sqrt{s-4m^2}} \begin{pmatrix} \cos 2\varepsilon e^{2i\delta_<} - 1 & i \sin 2\varepsilon e^{i(\delta_<+\delta_>)} \\ i \sin 2\varepsilon e^{i(\delta_<+\delta_>)} & \cos 2\varepsilon e^{2i\delta_>} - 1 \end{pmatrix}, \quad (3)$$

where m is a nucleon mass and ε is a mixing parameter. In Eq.(3) $\delta_< = \delta_{L=J-1}$, $\delta_> = \delta_{L=J+1}$ and l denotes $^S L_J$ states for simplicity. Expanding the T matrix into a series of \bar{p} -terms, according to [38]:

$$\bar{p} \cot \delta_l(s) = -\frac{1}{a_0^l} + \frac{r_0^l}{2} \bar{p}^2 + \mathcal{O}(\bar{p}^3), \quad (4)$$

where

$$\bar{p} \equiv |\bar{\mathbf{p}}| = \sqrt{s/4 - m^2} = \sqrt{mT_{\text{Lab}}/2} \quad (5)$$

is the on-mass-shell momentum, low-energy parameters, the scattering length a_0 and the effective range r_0 , can be derived.

The bound state of the two-particle system appears as a simple pole in the T matrix at $s = M_d^2$, with M_d being a mass of a bound state, in our case it is a deuteron. Thus, the Bethe-Salpeter equation for the BS amplitude Φ of the two-nucleon system with the total momentum J and its projection M has the following form:

$$\Phi^{JM}(p; P) = \frac{i}{(2\pi)^4} S_2(p; P) \int d^4k V(p, k; P) \Phi^{JM}(k; P), \quad (6)$$

The partial decomposed amplitude Φ can be written in the rest frame of the particles through the angular \mathcal{Y} and the radial ϕ parts as:

$$\Phi_{\alpha\beta}^{JM}(p; P_{(0)}) = \sum_a (\mathcal{Y}_{aM}(\mathbf{p}) U_C)_{\alpha\beta} \phi_a(p_0, |\mathbf{p}|; s). \quad (7)$$

Here U_C is the charge conjugation matrix. In the numerical calculations instead of the amplitude it is more convenient to use the vertex function Γ which is connected with the BS amplitude:

$$\Phi_{JM}(p; P) = S_2(p; P)\Gamma_{JM}(p; P), \quad (8)$$

so the radial parts of the BS amplitude ϕ and vertex function g are connected by the relation:

$$\phi_a(p_0, |\mathbf{p}|) = \sum_b S_{ab}(p_0, |\mathbf{p}|; s) g_b(p_0, |\mathbf{p}|). \quad (9)$$

To solve the equations for the T matrix and BS amplitude, we should use some assumption for the interaction kernel. In our case it is a separable kernel.

3. A separable kernel

We assume that the interaction kernel V conserves parity, total angular momentum J and its projection, and isotopic spin. Due to the tensor nuclear force, the orbital angular momentum L is not conserved. Moreover, the negative-energy two-nucleon states are omitted, which leads to the total spin S conservation. The partial-wave-decomposed BS equation is therefore reduced to the following form:

$$\begin{aligned} T_{l'l}(p'_0, |\mathbf{p}'|; p_0, |\mathbf{p}|; s) &= V_{l'l}(p'_0, |\mathbf{p}'|; p_0, |\mathbf{p}|; s) \\ &+ \frac{i}{4\pi^3} \sum_{l''} \int_{-\infty}^{+\infty} dk_0 \int_0^{\infty} k^2 dk |\mathbf{k}| \frac{V_{l'l''}(p'_0, |\mathbf{p}'|; k_0, |\mathbf{k}|; s) T_{l''l}(k_0, |\mathbf{k}|; p_0, |\mathbf{p}|; s)}{(\sqrt{s}/2 - E_{\mathbf{k}} + i\epsilon)^2 - k_0^2}. \end{aligned} \quad (10)$$

Supposing the separable (rank N) ansatz for the kernel of the NN interaction:

$$V_{l'l}(p'_0, |\mathbf{p}'|; p_0, |\mathbf{p}|; s) = \sum_{i,j=1}^N \lambda_{ij}(s) g_i^{[l']}(p'_0, |\mathbf{p}'|) g_j^{[l]}(p_0, |\mathbf{p}|), \quad (11)$$

where the form factors $g_j^{[l]}$ represent the model functions, we can obtain the solution of Eq.(11) in a similar separable form for the T matrix:

$$T_{l'l}(p'_0, |\mathbf{p}'|; p_0, |\mathbf{p}|; s) = \sum_{i,j=1}^N \tau_{ij}(s) g_i^{[l']}(p'_0, |\mathbf{p}'|) g_j^{[l]}(p_0, |\mathbf{p}|), \quad (12)$$

where

$$\tau_{ij}(s) = 1/(\lambda_{ij}^{-1}(s) + h_{ij}(s)), \quad (13)$$

$$h_{ij}(s) = -\frac{i}{4\pi^3} \sum_l \int dk_0 \int \mathbf{k}^2 d|\mathbf{k}| \frac{g_i^{[l]}(k_0, |\mathbf{k}|) g_j^{[l]}(k_0, |\mathbf{k}|)}{(\sqrt{s}/2 - E_{\mathbf{k}} + i\epsilon)^2 - k_0^2}, \quad (14)$$

$\lambda_{ij}(s)$ is a matrix of model parameters with the symmetry property:

$$\lambda_{ij}(s) = \lambda_{ji}(s). \quad (15)$$

Using the separable kernel in the form (11) and partially decomposed interaction kernel and vertex function we can represent the radial part of the latter as follows:

$$g_l(p_0, |\mathbf{p}|) = \sum_{i,j=1}^N \lambda_{ij}(s) g_i^{[l]}(p_0, |\mathbf{p}|) c_j(s), \quad (16)$$

where the integral equation (6) is reduced to a system of linear homogeneous equations for the coefficients $c_i(s)$:

$$c_i(s) - \sum_{k,j=1}^N h_{ik}(s) \lambda_{kj}(s) c_j(s) = 0. \quad (17)$$

The radial part of the BS amplitude has the form (see Eq.(9)):

$$\phi_l(p_0, |\mathbf{p}|) = \frac{g_l(p_0, |\mathbf{p}|)}{(M_d/2 - E_{\mathbf{p}} + i\epsilon)^2 - p_0^2}. \quad (18)$$

The form factors $g_i^{[l]}$ used in the separable representation of the interaction kernel (11) are obtained by a relativistic generalization of the initially non-relativistic Yamaguchi-type functions depending on the three-dimensional squared momentum $|\mathbf{p}|$. Methods of covariant relativistic generalizations of nonrelativistic form factors and the constructed form factors are discussed in the next section.

4. Construction of the kernel

We consider two types of a relativistic generalization of nonrelativistic Yamaguchi-type form factors [39] performing the following changes:

$$\mathbf{p}^2 \rightarrow -p^2 = -p_0^2 + \mathbf{p}^2 \quad (19)$$

$$\text{or} \quad \mathbf{p}^2 \rightarrow Q^2 : Q = p - \frac{P \cdot p}{s} P \quad (20)$$

and denote the resulting modified form factors of the constructed six-rank kernels by MY6 (19), MYQ6 (20). So high rank is necessary to describe phases for two waves and bound state characteristics in addition to usual low-energy parameters simultaneously. The form factors have the following form:

$$\begin{aligned} g_1^{[S]}(p) &= \frac{(p_{c1} - p_0^2 + \mathbf{p}^2)}{(p_0^2 - \mathbf{p}^2 - \beta_1^2)^2 + \alpha_1^4}, \\ g_2^{[S]}(p) &= \frac{(p_0^2 - \mathbf{p}^2)(p_{c2} - p_0^2 + \mathbf{p}^2)^2}{((p_0^2 - \mathbf{p}^2 - \beta_2^2)^2 + \alpha_2^4)^2}, \\ g_3^{[S]}(p) &= \frac{(p_0^2 - \mathbf{p}^2)^3(p_{c3} - p_0^2 + \mathbf{p}^2)^2}{((p_0^2 - \mathbf{p}^2 - \beta_3^2)^2 + \alpha_3^4)^3}, \end{aligned} \quad (21)$$

$$g_4^{[S]} = g_5^{[S]} = g_6^{[S]} = g_1^{[D]} = g_2^{[D]} = g_3^{[D]} = 0, \quad (22)$$

$$\begin{aligned} g_4^{[D]}(p) &= \frac{(p_0^2 - \mathbf{p}^2)(p_{c4} - p_0^2 + \mathbf{p}^2)^2}{((p_0^2 - \mathbf{p}^2 - \beta_{41}^2)^2 + \alpha_{41}^4)((p_0^2 - \mathbf{p}^2 - \beta_{42}^2)^2 + \alpha_{42}^4)}, \\ g_5^{[D]}(p) &= \frac{(p_0^2 - \mathbf{p}^2)}{(p_0^2 - \mathbf{p}^2 - \beta_5^2)^2 + \alpha_5^4}, \\ g_6^{[D]}(p) &= \frac{(p_0^2 - \mathbf{p}^2 - p_{c6})(p_0^2 - \mathbf{p}^2)^4}{((p_0^2 - \mathbf{p}^2 - \beta_{61}^2)^2 + \alpha_{61}^4)((p_0^2 - \mathbf{p}^2 - \beta_{62}^2)^2 + \alpha_{62}^4)^2}. \end{aligned} \quad (23)$$

The functions for the kernel MYQ6 can be obtained from (21)-(23) by the change $p^2 \rightarrow Q^2$. The detailed discussion of properties of the presented form factors can be found in [32]-[34].

Due to the structure of the kernel, Eqs.(21)-(23), the matrix $H = \{h_{ij}\}$ (14) can be written as

$$H(s) = \begin{pmatrix} h_{11}(s) & h_{12}(s) & h_{13}(s) & 0 & 0 & 0 \\ h_{12}(s) & h_{22}(s) & h_{23}(s) & 0 & 0 & 0 \\ h_{13}(s) & h_{23}(s) & h_{33}(s) & 0 & 0 & 0 \\ 0 & 0 & 0 & h_{44}(s) & h_{45}(s) & h_{46}(s) \\ 0 & 0 & 0 & h_{45}(s) & h_{55}(s) & h_{56}(s) \\ 0 & 0 & 0 & h_{46}(s) & h_{56}(s) & h_{66}(s) \end{pmatrix}. \quad (24)$$

The solution of the BS equation for the radial parts of the vertex function can be expressed through the introduced form factors with the help of Eqs.(9), (16), (17). To fix the coefficients c_i which are solutions of a system of linear homogeneous equations we use the normalization condition for the 3S_1 and 3D_1 states:

$$p_S + p_D = 1, \quad (25)$$

where the pseudoprobabilities of these waves are introduced:

$$p_l = \frac{i}{2M_d(2\pi)^4} \int dp_0 \int \mathbf{p}^2 d|\mathbf{p}| \frac{(E_{\mathbf{p}} - M_d/2)[g_l(p_0, |\mathbf{p}|)]^2}{((M_d/2 - E_{\mathbf{p}} + i\epsilon)^2 - p_0^2)^2}, \quad (26)$$

The resulting coefficients c_i are presented in Table 1.

The half-off-shell behavior of the kernel is controlled by the Noyes-Kowalski function [35, 36]

$$f_{l'l}(p; \bar{p}) = \frac{T_{l'l}(0, |\mathbf{p}|; 0, |\bar{\mathbf{p}}|; s)}{T_{l'l}(0, |\bar{\mathbf{p}}|; 0, |\bar{\mathbf{p}}|; s)} \quad (27)$$

and compared with the Paris [18] potential and relativistic Graz II kernel [29]. Here $\bar{\mathbf{p}}$ (5) is the on-shell and \mathbf{p} is the off-shell momenta, respectively. It should be noted that there are three different variants of the relativistic Graz II kernel differed by the D wave probability. We choose the variant with the $p_D = 5\%$.

We also see to the deuteron asymptotic D/S ratio

$$\rho_{D/S} = \frac{g_{3D_1^+}(0, p^*)}{g_{3S_1^+}(0, p^*)}, \quad (28)$$

where $p^{*2} = -mE_d$, and the deuteron magnetic moment μ_d .

Table 1: Coefficients c_i .

	MY6	MYQ6
c_1	0.0486061704	0.0704040072
c_2	0.00225058402	0.00453017913
c_3	-0.00671506834	-0.171434026
c_4	-0.019764894	0.0080399654
c_5	0.00277839389	0.00618413506
c_6	-0.304144129	0.0682392337

5. Calculations and results

Using the np scattering data we analyze the parameters of the separable kernels. A pole in the T matrix at the mass of the bound state M_d :

$$\det |\tau_{ij}^{-1}(s = M_d^2)| = 0 \quad (29)$$

is taken into account by using the relation

$$\lambda_{ij}(s) = \frac{\bar{\lambda}_{ij}}{s - m_0^2}. \quad (30)$$

The parameter m_0 is chosen to satisfy the following condition:

$$\bar{\lambda}_{ij}^{-1}(s - m_0^2) + \Re h_{ij}(M_d^2) = 0, \quad (31)$$

where $M_d = (2m - E_d)$ and E_d is the energy of the deuteron.

The calculation of the parameters is done by using Eqs.(3),(4) and expressions given to reproduce experimental values for all available data from the SAID program (<http://gwdac.phys.gwu.edu>) for phase shifts. The low-energy scattering parameters are taken from [40].

The calculations are performed using the Wick rotation [41]. All integrals are calculated numerically with the technique elaborated in the paper [42].

The introduced parameters of the kernel are found from the minimization of the χ^2 function. The asymptotic ratio $\rho_{D/S}$ is also taken into account in the minimization procedure. The phase shifts for S and D waves are both included in one minimization function:

$$\begin{aligned} \chi^2 = & \sum_{i=1}^n (\delta_{<}^{\text{exp}}(s_i) - \delta_{<}(s_i))^2 / (\Delta \delta_{<}^{\text{exp}}(s_i))^2 + (\delta_{>}^{\text{exp}}(s_i) - \delta_{>}(s_i))^2 / (\Delta \delta_{>}^{\text{exp}}(s_i))^2 \\ & + (a^{\text{exp}} - a)^2 / (\Delta a^{\text{exp}})^2 + (\rho_{D/S}^{\text{exp}} - \rho_{D/S})^2 / (\Delta \rho_{D/S}^{\text{exp}})^2. \end{aligned} \quad (32)$$

Here n is a number of experimental points.

The effective range r_0 is calculated via the obtained parameters and compared with the experimental value r_0^{exp} .

The calculated parameters of the constructed kernels are listed in Tables 2 and 3. In Table 4, the calculated low-energy scattering parameters and deuteron characteristics are compared with the corresponding experimental values and other models (Graz II [29], Paris [18], CD-Bonn [43]).

In Figs.1,2, the results of the phase shifts calculations are compared with experimental data and, in addition to aforesaid theoretical models, with the alternative description by SP07 [44]. The mixing parameter is pictured in Fig.3. In this specific case only nonrelativistic Graz II [24] kernel (denoted by Graz II (NR)) is considered as an example of comparison with a separable model because calculations with the relativistic kernel [29] are impossible to perform at high energies as it was discussed in [34].

The obtained components of the Noyes-Kowalski function are presented in Figs.4-7. The S - and D -state wave functions $\phi(\bar{p}_0, \mathbf{p})$ where $\bar{p}_0 = M_d/2 - E_{\mathbf{p}}$ [48] are given in Fig.8 and 9, respectively, and compared with the corresponding relativistic and nonrelativistic Graz II kernels and the Paris potential.

As an example of application of the elaborated kernel, in Figs.10-12 the results of calculations of cross sections for the deuteron electrodisintegration within the relativistic plane-wave impulse approximation are presented. We compare our new results for the differential cross section with ones obtained earlier [47] using the relativistic Graz II [29] kernel for three cases differed by given kinematical conditions [49, 50].

Table 2: Parameters of the six-rank kernel with modified (19) Yamaguchi functions MY6.

MY6			
$\bar{\lambda}_{11}$ (GeV ²)	-126.823	β_1 (GeV)	0.1000189
$\bar{\lambda}_{12}$ (GeV ²)	-1627.106	β_2 (GeV)	1.2089089
$\bar{\lambda}_{13}$ (GeV ²)	-78.78723	β_3 (GeV)	0.3884728
$\bar{\lambda}_{14}$ (GeV ²)	1255.789	β_{41} (GeV)	0.1617235
$\bar{\lambda}_{15}$ (GeV ²)	1920.741	β_{42} (GeV)	1.0569099
$\bar{\lambda}_{16}$ (GeV ²)	23.25852	β_5 (GeV)	0.5975024
$\bar{\lambda}_{22}$ (GeV ²)	-1507.037	β_{61} (GeV)	0.1000189
$\bar{\lambda}_{23}$ (GeV ²)	-202.4665	β_{62} (GeV)	0.2562457
$\bar{\lambda}_{24}$ (GeV ²)	-1211.809	α_1 (GeV)	1.7190386
$\bar{\lambda}_{25}$ (GeV ²)	19296.73	α_2 (GeV)	1.1342682
$\bar{\lambda}_{26}$ (GeV ²)	19.71478	α_3 (GeV)	0.3825411
$\bar{\lambda}_{33}$ (GeV ²)	-4.911057	α_{41} (GeV)	0.1143112
$\bar{\lambda}_{34}$ (GeV ²)	52.90785	α_{42} (GeV)	1.9584773
$\bar{\lambda}_{35}$ (GeV ²)	-557.975	α_5 (GeV)	10.71719
$\bar{\lambda}_{36}$ (GeV ²)	-5.781583	α_{61} (GeV)	0.1743705
$\bar{\lambda}_{44}$ (GeV ²)	2388.451	α_{62} (GeV)	0.3825411
$\bar{\lambda}_{45}$ (GeV ²)	1481.914	p_{c1} (GeV ²)	-3.947706
$\bar{\lambda}_{46}$ (GeV ²)	23.63605	p_{c2} (GeV ²)	-29.997902
$\bar{\lambda}_{55}$ (GeV ²)	-47615.28	p_{c3} (GeV ²)	3.9076391
$\bar{\lambda}_{56}$ (GeV ²)	314.5085	p_{c4} (GeV ²)	0.5632583
$\bar{\lambda}_{66}$ (GeV ²)	1.135512	p_{c6} (GeV ²)	0.278038

Table 3: Parameters of the six-rank kernel with modified (20) Yamaguchi functions MYQ6.

MYQ6			
$\bar{\lambda}_{11}$ (GeV ²)	-10.574	β_1 (GeV)	0.100019
$\bar{\lambda}_{12}$ (GeV ²)	-3498.482	β_2 (GeV)	0.5978559
$\bar{\lambda}_{13}$ (GeV ²)	2.031008	β_3 (GeV)	0.431291
$\bar{\lambda}_{14}$ (GeV ²)	98.12	β_{41} (GeV)	0.210503
$\bar{\lambda}_{15}$ (GeV ²)	31.318	β_{42} (GeV)	0.1001783
$\bar{\lambda}_{16}$ (GeV ²)	-30.813	β_5 (GeV)	5.5725
$\bar{\lambda}_{22}$ (GeV ²)	10548.08	β_{61} (GeV)	0.1120488
$\bar{\lambda}_{23}$ (GeV ²)	-76.928	β_{62} (GeV)	0.4489458
$\bar{\lambda}_{24}$ (GeV ²)	-3720.413	α_1 (GeV)	1.468872
$\bar{\lambda}_{25}$ (GeV ²)	37427.57	α_2 (GeV)	1.09121
$\bar{\lambda}_{26}$ (GeV ²)	-208.697	α_3 (GeV)	0.7449097
$\bar{\lambda}_{33}$ (GeV ²)	0.77	α_{41} (GeV)	0.1
$\bar{\lambda}_{34}$ (GeV ²)	-22.51814	α_{42} (GeV)	1.945662
$\bar{\lambda}_{35}$ (GeV ²)	-84.478	α_5 (GeV)	4.08
$\bar{\lambda}_{36}$ (GeV ²)	2.1435	α_{61} (GeV)	0.2058123
$\bar{\lambda}_{44}$ (GeV ²)	895.2475	α_{62} (GeV)	0.7052189
$\bar{\lambda}_{45}$ (GeV ²)	286.5565	p_{c1} (GeV ²)	-4.2035
$\bar{\lambda}_{46}$ (GeV ²)	19.419	p_{c2} (GeV ²)	-13.82
$\bar{\lambda}_{55}$ (GeV ²)	-32435.14	p_{c3} (GeV ²)	9.574
$\bar{\lambda}_{56}$ (GeV ²)	-705.156	p_{c4} (GeV ²)	1.152
$\bar{\lambda}_{66}$ (GeV ²)	-21.792	p_{c6} (GeV ²)	-0.4527

Table 4: The low-energy scattering parameters for the triplet ${}^3S_1^+ - {}^3D_1^+$ state and the deuteron characteristics.

	a_{0t} (fm)	r_{0t} (fm)	p_D (%)	E_d (MeV)	$\rho_{D/S}$	μ_d ($e/2m$)
MY6	5.42	1.800	4.92	2.2246	0.0255	0.8500 ^a
MYQ6	5.42	1.768	4.65	2.2246	0.0259	0.8535 ^a
Graz II	5.42	1.779	5	2.2254	0.0269	0.8512
Paris	5.43	1.770	5.77	2.2249	0.0261	0.8469
CD-Bonn	5.4196	1.751	4.85	2.2246	0.0256	0.8522
Exp.	5.424(4)	1.759(5)	4-7	2.224644(46)	0.0256(4) ^b	0.8574 ^c

^a Calculated within the relativistic impulse approximation with the positive-energy partial states only.

^b Ref. [45].

^c Ref. [46].

6. Discussion and conclusions

First step in construction of the kernel is the description of on-mass-shell characteristics, like phase shifts, low-energy characteristics, and the mixing parameter. In Figs.1,2, the results of our calculations of phase shifts for the ${}^3S_1^+$ and ${}^3D_1^+$ waves are presented. Figure 1 demonstrates that the ${}^3S_1^+$ partial state is well described by both MY6 and MYQ6 parametrizations for all experimental data. The Graz II works for $T_{\text{Lab}} \leq 0.4$ GeV. For the ${}^3D_1^+$ state MY6 and MYQ6 provide a good description of existing data. Graz II shows only some correspondence with the data for $T_{\text{Lab}} \leq 0.4$ GeV. SP07 is good for all experimental data. CD-Bonn was constructed for $T_{\text{Lab}} \leq 350$ MeV and is perfect in this region. Its behavior means that other models should be used for higher energies. Our kernel is intended to perform calculations exactly in this case.

The problem of simultaneous description of phase shifts for two partial states, the mixing parameter and low-energy and deuteron characteristics is worthy of a special discussion. This subject was considered in detail in [24]. The authors found out that an attempt to describe well the mixing parameter together with other observables leads to very bad results for the low-energy and deuteron parameters. They become too small in comparison with permissible values, in particular $p_D \lesssim 1\%$. Performing our numerical investigations we discovered the same properties. In most cases there is

no possibility to reproduce phase shifts, low-energy parameters, and mixing parameter simultaneously. A certain advance was achieved in the CD-Bonn potential model where the mixing parameter behavior looks very good for kinetic energies till about 350 MeV for Nijmegen group analysis [51]. Although there are SAID group data [44] which differ from Nijmegen group ones this is the best result for the moment. However, taking into account this discrepancy in the analysis of the experimental data for the mixing parameter we restrict ourselves to the description of all observables but ε . At the same time, for completeness we present the obtained results for ε along with the results of all other discussed models (Fig.3). It can be seen that both our versions do not work at all like Graz II model which also does not give any agreement with the data. SP07 agrees with the experiment in a whole energy range.

The half-off-shell behavior characterized by the Noyes-Kowalski function (27) was not fitted in any special way, it was simply calculated as it is. In Figs.4-7, all components of this function are presented. The obtained MY6 and MYQ6 functions are similar but not identical to the Graz II potential functions. The same can be said about diagonal components of the function for the realistic Paris potential. Whereas the difference for non-diagonal components is significant. In addition, MY6 modification is not identical to MYQ6 one. This difference should affect on observables defined by the half-off-shell behavior of the described interaction like, for example, various polarizations [52]. However, as it is demonstrated below some results are practically identical for observables which depend mostly on the on-shell behavior of the interaction.

As any other phenomenological kernel ours can describe on-shell characteristics quite easily. However the description of the deuteron is not limited only by phase shifts and low-energy observables. It is also important deuteron wave function and off-shell behavior to be considered properly. Therefore in our calculations we take into account features of wave functions corresponding to $^3S_1^+$ and $^3D_1^+$ parts. In Figs.8,9, it is shown that the obtained functions are similar to other discussed models in the energy region where their properties play a key role.

As an example of using our kernel we calculate the differential cross sections [47] within the simplest relativistic plane-wave impulse approximation for various kinematical conditions [49, 50] and compare them with the corresponding relativistic Graz II model [29] calculations. From Figs.10-12, it can be seen that the presented results begin to differ only when the influ-

ence of the D wave increases. However, to make a conclusion it is necessary other effects, like the final state interaction (FSI) and two-body currents, to be taken into account. It was impossible before because of problems with calculations as it was discussed in [34]. Now these difficulties are obviated and it is planned to perform calculations of observables with FSI using the presented kernel and the results of our previous work [34] in near future.

In conclusion it can be said that the constructed six-rank kernel was successfully used for the description of the on-shell and off-shell characteristics of the deuteron. A good agreement with results of other models which work at low energies for phase shifts, low-energy parameters, deuteron wave function was achieved. The demonstrated half-off-shell behavior is similar to corresponding Graz II model. The presented kernel can be used in calculations of various reactions with the deuteron, e.g. the deuteron photo- and electrodisintegration etc. It is also interesting to investigate deuteron elastic form factors using this new kernel. However it is a subject of a separate work.

Additional parameters α provide integrands containing form factors of the separable kernel do not have poles for \mathbf{p} component. Therefore, in particular, using this type of kernel will make numerical calculations of the electrodisintegration far from the threshold possible without resorting quasipotential or nonrelativistic models. Comparison with other separable and realistic potential models allow us to demonstrate merits of our kernel. For example, the Bonn potential, which was constructed for $T_{\text{Lab}} \leq 350$ MeV and works in this energy interval very well, is difficult to continue to higher energies. As for the Graz II kernel the increase of energies of the considered particles is impossible in principle. On the contrary, our kernel has no these limitations. We do not describe the mixing parameter nevertheless all low-energy and deuteron characteristics are reproduced well and the results for phase shifts cover the whole energy region and are of high quality. Finally we have no insuperable obstacles in calculations and there is an opportunity to improve the model in future.

7. Acknowledgements

We wish to thank Drs. A.A. Goy, D.V. Shulga, K.Yu. Kazakov and Prof. G. Rupp for their interest in the present work and fruitful discussions. S.G.B. and V.V.B. thank the National Taiwan University for their warm hospitality.

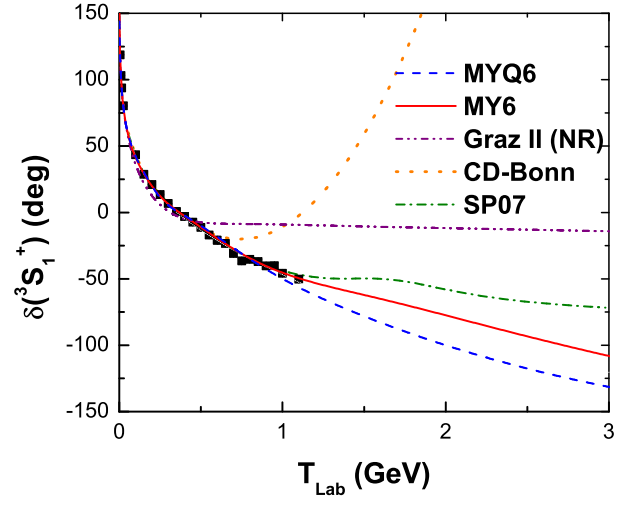


Figure 1: Phase shifts for the $^3S_1^+$ wave.

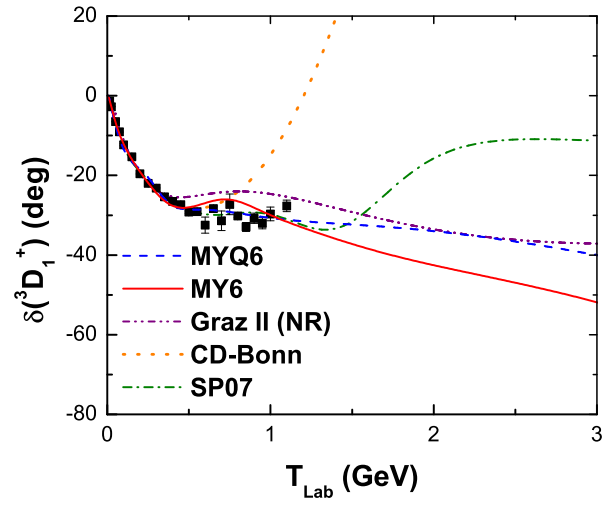


Figure 2: Phase shifts for the $^3D_1^+$ wave.

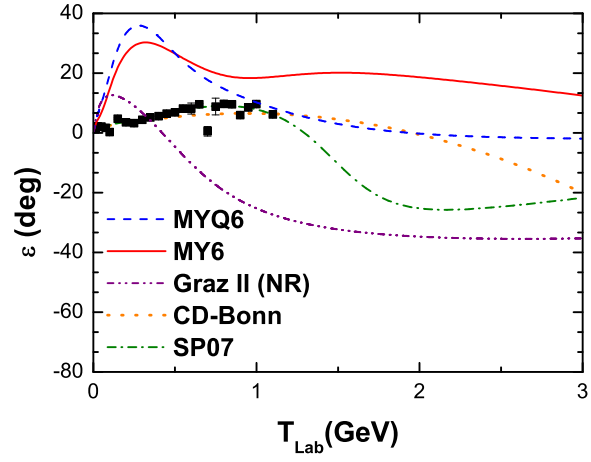


Figure 3: The mixing parameter.

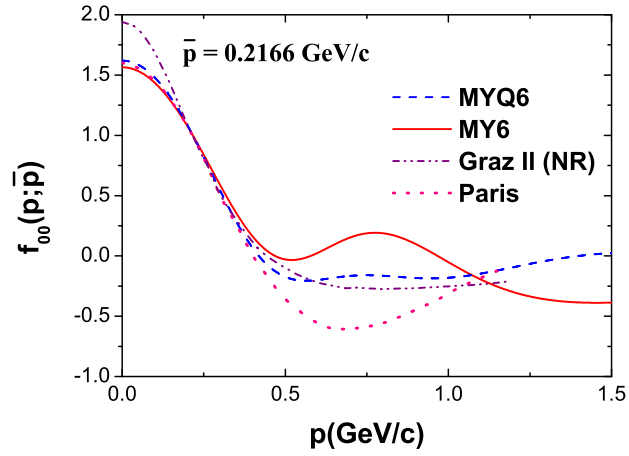


Figure 4: Noyes-Kowalski function f_{00} .

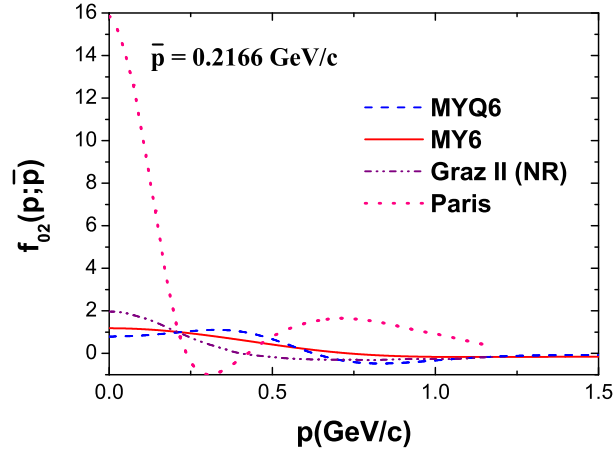


Figure 5: Noyes-Kowalski function f_{02} .

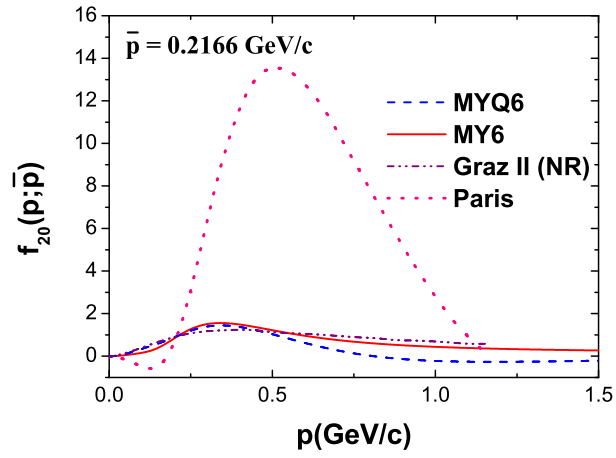


Figure 6: Noyes-Kowalski function f_{20} .

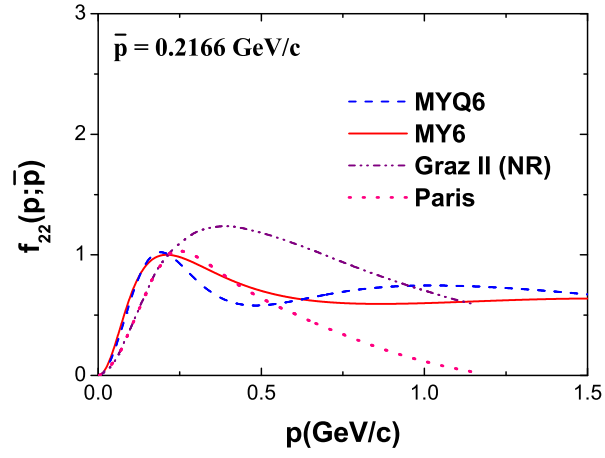


Figure 7: Noyes-Kowalski function f_{22} .

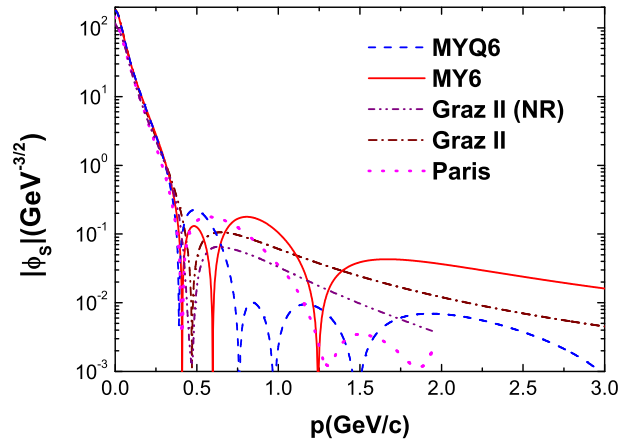


Figure 8: Wave function for the $^3S_1^+$ partial state.

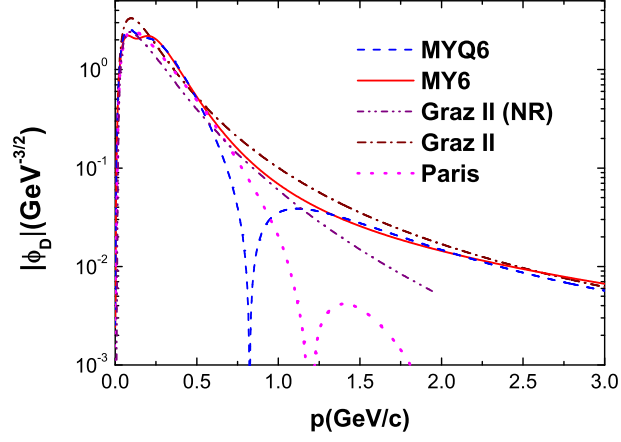


Figure 9: Wave function for the ${}^3D_1^+$ partial state.

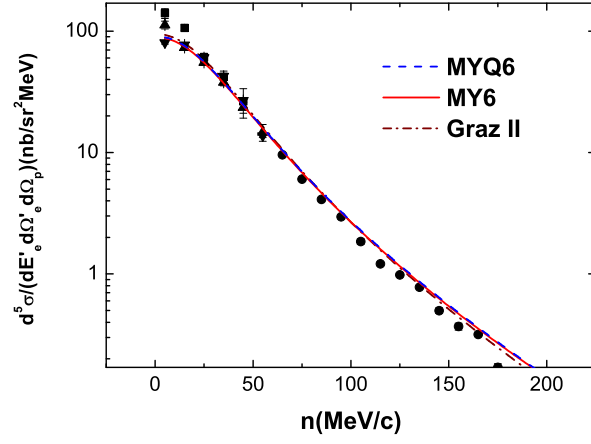


Figure 10: Cross section for the $e(d,e'n)p$ reaction, kinematical conditions set I [49]. E_e is the energy of the initial electron, p is the final proton momentum. The detailed discussion of the considered observable can be found in [47].

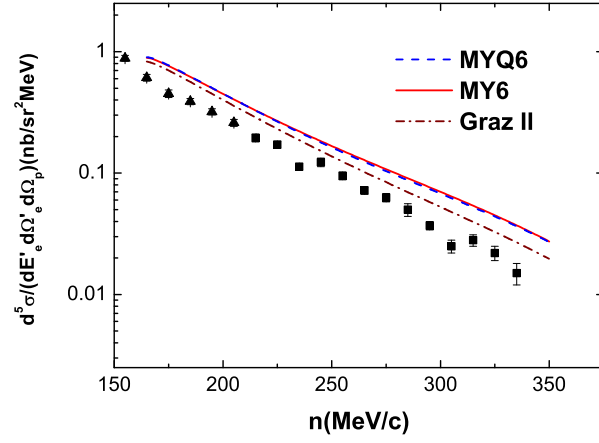


Figure 11: Cross section for the kinematical conditions set II [49]. See also the caption of Fig.10.

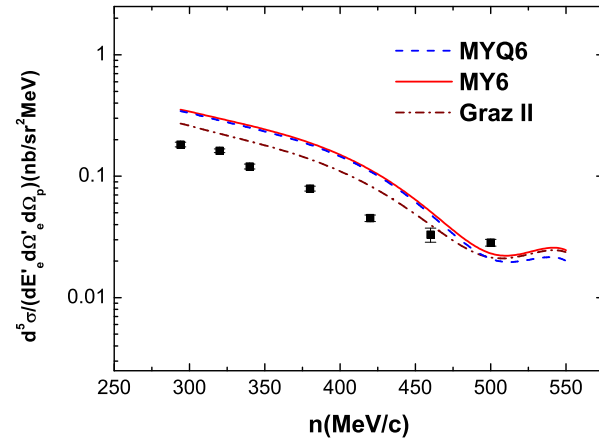


Figure 12: Cross section for the kinematical conditions [50]. See also the caption of Fig.10.

References

- [1] G.E. Brown and A.D. Jackson, RX-707 (NORDITA).
- [2] F. Gross, Modern Topics in Electron Scattering, World Scientific, 1991.
- [3] V. Pascalutsa, J.A. Tjon, Phys. Rev. C 61 (2000) 054003, nucl-th/0003050.
- [4] J.F. Mathiot, Nucl. Phys. A 412 (1984) 201.
- [5] R.F. Wagenbrunn, W. Plessas, Few Body Syst. Suppl. 8 (1995) 181.
- [6] T. Wilbois, G. Beck, H. Arenhovel, Few Body Syst. 15 (1993) 39.
- [7] J. Carbonell, B. Desplanques, V.A. Karmanov, J.F. Mathiot, Phys. Rept. 300 (1998) 215, nucl-th/9804029.
- [8] M. Gari, H. Hyuga, Z. Phys. A 277 (1976) 29.
- [9] W.Y.P. Hwang, T.W. Donnelly, Phys. Rev. C 33 (1986) 1381.
- [10] W.Y.P. Hwang, G.E. Walker, Annals Phys. 159 (1985) 118.
- [11] S.D. Kurgalin, Yu.M. Chuvilsky, Sov. J. Nucl. Phys. 49 (1989) 79.
- [12] A.Yu. Illarionov, G.I. Lykasov, Phys. Rev. C 64 (2001) 044004.
- [13] A. Faessler, V.I. Kukulin, M.A. Shikhalev, Annals Phys. 320 (2005) 71, nucl-th/0505026.
- [14] D. Chiladze *et al.* Eur. Phys. J. A 40 (2009) 23.
- [15] A.F. Krutov, V.E. Troitsky, Phys. Part. Nucl. 40 (2009) 136.
- [16] L.S. Azhgirey, Phys. Part. Nucl. 37, No. 4 (2006) 1011.
- [17] S.G. Bondarenko, V.V. Burov, A.V. Molochkov, G.I. Smirnov, H. Toki, Prog. Part. Nucl. Phys. 48 (2002) 449, nucl-th/0203069.
- [18] M. Lacombe *et al.*, Phys. Rev. C 21 (1980) 861.
- [19] R. Machleidt, K. Holinde, Proceedings, Few Body Problems In Physics, Vol. 2 (1984) 79.

- [20] L. Crepinsek, H. Oberhummer, W. Plessas, H. Zingl, *Acta Phys. Austriaca* 39 (1974) 345.
- [21] L. Crepinsek, C.B. Lang, H. Oberhummer, W. Plessas, H.F.K. Zingl, *Acta Phys. Austriaca* 42 (1975) 139.
- [22] M.I. Haftel, *Phys. Rev. C* 14 (1976) 698.
- [23] N. Giraud, Y. Avishai, C. Fayard, G.H. Lamot, *Phys. Rev. C* 19 (1979) 465.
- [24] L. Mathelitsch, W. Plessas, M. Schweiger, *Phys. Rev. C* 26 (1982) 65.
- [25] J. Haidenbauer, W. Plessas, *Phys. Rev. C* 30 (1984) 1822.
- [26] J. Haidenbauer, Y. Koike, W. Plessas, *Phys. Rev. C* 33 (1986) 439.
- [27] R.V. Reid, Jr., *Ann. Phys.* 50 (1968) 411.
- [28] D.J. Ernst, C.M. Shakin, R.M. Thaler, *Phys. Rev. C* 8 (1973) 46.
- [29] G. Rupp, J.A. Tjon, *Phys. Rev. C* 41 (1990) 472.
- [30] K. Schwarz, J. Frohlich, H.F.K. Zingl, *Acta Phys. Austriaca* 53 (1981) 191.
- [31] S.G. Bondarenko, V.V. Burov, K.Y. Kazakov, D.V. Shulga, *Phys. Part. Nucl. Lett.* 1 (2004) 178, nucl-th/0402056.
- [32] S.G. Bondarenko, V.V. Burov, W.-Y. Pauchy Hwang, E.P. Rogochaya, *JETP Lett.* 87 (2008) 753, 0804.3525.
- [33] S.G. Bondarenko, V.V. Burov, E.P. Rogochaya, Y. Yanev, 0806.4866 (2008).
- [34] S.G. Bondarenko, V.V. Burov, W.-Y. Pauchy Hwang, E.P. Rogochaya, *Nucl. Phys. A* 832 (2010) 233.
- [35] H.P. Noyes, *Phys. Rev. Lett.* 15 (1965) 538.
- [36] K.L. Kowalski, *Phys. Rev. Lett.* 15 (1965) 798.
- [37] E.E. Salpeter, H.A. Bethe, *Phys. Rev.* 84 (1951) 1232.

- [38] H.A. Bethe, Phys. Rev. 76 (1949) 38.
- [39] Y. Yamaguchi, Phys. Rev. 95 (1954) 1628;
Y. Yamaguchi, Y. Yamaguchi, Phys. Rev. 95 (1954) 1635.
- [40] O. Dumbrajs *et al.*, Nucl. Phys. B 216 (1983) 277.
- [41] T.D. Lee, G.C. Wick, Nucl. Phys. B 9 (1969) 209.
- [42] J. Fleischer, J.A. Tjon, Nucl. Phys. B 84 (1975) 375.
- [43] R. Machleidt, Phys. Rev. C 63 (2001) 024001.
- [44] R.A. Arndt, W.J. Briscoe, I.I. Strakovsky, R.L. Workman, Phys. Rev. C 76 (2007) 025209, 0706.2195.
- [45] N.L. Rodning, L.D. Knutson, Phys. Rev. C 41 (1990) 898.
- [46] N. Honzawa, S. Ishida, Phys. Rev. C 45 (1992) 47.
- [47] S.G. Bondarenko, V.V. Burov, E.P. Rogochaya, A.A. Goy, Phys. Atom. Nucl. 70 (2007) 2054.
- [48] S.G. Bondarenko, V.V. Burov, M. Beyer, S.M. Dorkin, Phys. Rev. C 58 (1998) 3143.
- [49] A. Bussiere *et al.*, Nucl. Phys. A 365 (1981) 349.
- [50] S. Turck-Chieze *et al.*, Phys. Lett. B 142 (1984) 145.
- [51] V.G.J. Stoks, R.A.M. Kompl, M.C.M. Rentmeester, J.J. de Swart, Phys. Rev. C 48 (1993) 792.
- [52] B. Loiseau, L. Mathelitsch, W. Plessas, K. Schwarz, Phys. Rev. C 32 (1985) 2165.